European Journal of Mechanics A/Solids 41 (2013) 58–69

Contents lists available at SciVerse ScienceDirect

European Journal of Mechanics A/Solids

journal homepage: www.elsevier.com/locate/ejmsol

Laminated beam analysis by polynomial, trigonometric, exponential and zig-zag theories

E. Carrera, M. Filippi*, E. Zappino

Department of Mechanics and Aerospace Engineering, Politecnico di Torino, Corso Duca Degli Abruzzi 24, 10129 Torino, Italy

ARTICLE INFO

Article history:
Received 5 December 2012
Accepted 19 February 2013
Available online 14 March 2013

Keywords:
Beams
Finite Element method
Higher-order theories
Composites Structures

ABSTRACT

A number of refined beam theories are discussed in this paper. These theories were obtained by expanding the unknown displacement variables over the beam section axes by adopting Taylor's polynomials, trigonometric series, exponential, hyperbolic and zig-zag functions. The Finite Element method is used to derive governing equations in weak form. By using the Unified Formulation introduced by the first author, these equations are written in terms of a small number of fundamental nuclei, whose forms do not depend on the expansions used. The results from the different models considered are compared in terms of displacements, stress and degrees of freedom (DOFs). Mechanical tests for thick laminated beams are presented in order to evaluate the capability of the finite elements. They show that the use of various different functions can improve the performance of the higher-order theories by yielding satisfactory results with a low computational cost.

1. Introduction

Composite materials are widely used in many branches of engineering, for example in the aerospace, automobile, nuclear and biomedical fields. The increase in the use of these materials is due to their attractive properties of strength, stiffness and lightness. On the other side, the behavior of composite structures is governed by a wider number of parameters than conventional materials and, hence, the study of their mechanics becomes difficult. Furthermore new problems arise such as the delamination and a reliable structural model becomes essential in order to predict the distributions of normal and transverse shear stresses.

The classical beam model introduced by Euler and Bernoulli (Euler, 1744) yields very poor results when dealing with moderately deep laminated beams, since the shear effects on the deformation of the cross-section are disregarded. In order to overcome this limitation, Timoshenko (Timoshenko and Goodier, 1970; Timoshenko, 1921) provided his well-known theory, in which he assumed a constant distribution of shear deformation over the cross-section. The major drawback is that this theory requires the use of the shear correction factor, which is a problem dependent parameter. Hence, in the light of these considerations, the classical and first-order shear deformation theories are inadequate to analyze laminated composite beams and, therefore, in order to obtain accurate solutions a wide variety of higher-order models have been conceived. Reddy (1984) presented a plate theory which provides a parabolic distribution of the transverse shear strains ensuring that the transverse shear stresses are null on the top and bottom surfaces. By using this model, exact closed-form solutions for static, buckling and dynamic analyses of cross-ply laminated beams with arbitrary boundary conditions were presented in Khdeir et al. (1997a,b), and Khdeir (1996). On the other side, Surana and Nguyen (1990) presented an interesting two-dimensional curved beam element in which Lagrange's polynomials are used to obtain several higher-order theories. The hierarchical property of the formulation makes it possible for the displacement expansion in the transverse direction to be of arbitrary polynomial order p, thereby permitting strains of at least order $(p-1)$. On the other hand, in accordance with Matsunaga's theory (Matsunaga, 2002), the displacement components can be expanded into power series of the depth coordinate (z). In Matsunaga's paper, axial stresses were computed through the constitutive relations, whereas the transverse shear stresses were determined by integration of the three-dimensional equilibrium equations. On the other hand in Rao et al. (2001), Kameswara Rao put the displacement components in the cross-section plane using Taylor's series expansion computing the free vibrations of laminated beams by adopting a mixed theory. Mantari et al. (2012) expressed the displacement components of laminated plates by adopting a combination of exponential and

* Corresponding author. Tel.: +39 (0)11 090 6870; fax: +39 (0)11 090 6899.
E-mail addresses: erasmo.carrera@polito.it (E. Carrera), matteo.filippi@polito.it, fil.matteo@live.it (M. Filippi), enrico.zappino@polito.it (E. Zappino).

0997-7538/$ – see front matter © 2013 Elsevier Masson SAS. All rights reserved.
http://dx.doi.org/10.1016/j.euromechsol.2013.02.006

trigonometric functions, whereas Karama et al. (2003) studied the mechanical behavior of composite beams by adopting an exponential function ensuring the continuity of the shear stresses with Ossadzow's kinematics. Recently, Vidal et al. (2012) proposed the approximation of the displacement field as a sum of separated functions of axial and transverse coordinate by adopting the Proper Generalized Decomposition procedure, whereas Li et al. (Jun and Hongxing, 2009) used the Dynamic Stiffness Matrix and a trigonometric shear deformation theory for solving the equations of motion of laminated beams. Furthermore, Grover et al. (2013) studied the stability and the static behavior of laminated and sandwich plates by using an inverse hyperbolic shear deformation theory providing a closed-form solution for a simply supported symmetric plates. All the aforementioned theories are based on the equivalent single layer approach. The continuity of the shear strains at interfaces leads to a discontinuous distribution of shear stresses (if they are computed through the constitutive equations) that represents the major limit of this kind of models. To avoid this shortcoming, many researchers have adopted the layer-wise approach. For example, Shimpi and Ghugal presented a new layer-wise trigonometric model for two-layered cross-ply beams (Shimpi and Ghugal, 2001). The main feature of this theory is that the shear stresses are derived directly from the constitutive equations satisfying both the shear-stress-free condition at the free surfaces of the beam and the condition of continuity of the shear stresses at the interface. This model represents a layer-dependent theory in which the number of unknowns depends on the number of layers that constitute the structure. On the same topic, Tahani (2007) proposed two theories for analyzing the static and dynamic behavior of the laminated beams. In the first case, a layer-wise plate theory was adapted to beams, whereas the second model was obtained following a simple procedure similar to the one used in the development of plate and shell theories. Unfortunately, when the number of layers increases, the layer-wise approach becomes unfavorable because it is too expensive in terms of computational cost. To overcome this problem, many researchers have introduced layer independent theories in which zig-zag or Heaviside's functions are widely used. Murakami (1986) was the first to introduce a zig-zag function into Reissner's new mixed variational principle to develop a plate theory (for a complete review of Murakami's zig-zag method, see Carrera, 2003a). Vidal and Polit (2008, 2009) presented a refined sine model by providing a Heaviside function for each layer to satisfy the continuity conditions for both displacements and transverse shear stress and the free conditions of the upper and lower surfaces. Subsequently, the same authors introduced Murakami's zig-zag function in the sine model (Vidal and Polit, 2011) so as to take into account the discontinuity of the first derivative of the displacements. A further example is Oñate's paper (Onate et al., 2012), where a new linear two-nodes beam element is evaluated based on the combination of classical Timoshenko theory and the refined zig-zag kinematics proposed by Tessler et al. (2009).

It is clear that many attempts have been made (see Kapania and Raciti, 1989; Shimpi and Ghugal, 2002) in order to give a general and reliable theory able to capture every aspect of the complex nature of the composite materials. In the present paper, a great variety of higher-order theories are tested for studying the static behavior of laminated beams. These theories derive from Carrera's Unified Formulation (CUF), that offers a procedure to obtain refined structural models. The procedure makes it possible to consider the order and the types of theories as free input parameters. CUF was first developed for plate and shell models. For instance, in Carrera (2002, 2003b), Carrera provided a comprehensive description of possible approaches to plate and shell laminated structures and introduced the Unified Formulation to obtain several models based on displacements and transverse stress assumptions. Furthermore, Finite Element implementations were presented by detailing the matrices of the elements. Ballhause et al. (2004) investigated the static and dynamic behavior of multilayered plates embedding piezo-layers by using CUF. The results show that Unified Formulation is able to lead to a quasi-3D description of global and local characteristics of the piezoelectric plates. Further assessments are presented in Carrera (2004), in which the vibrational free response of homogenous and multilayered simply supported plates is evaluated. Carrera et al. (2007) used CUF to analyze multifield problems related to multilayered plates subjected to thermal, mechanical and electric loads. In Carrera et al. (2008) the same analyses were performed by adding of a magnetic load.

Recently, CUF has been extended to the beam model. Carrera and Giunta tested the performance of higher-order theories, by using N-order Taylor type expansions (TE) of the section coordinates in order to define the displacement variables (Carrera and Giunta, 2010). In that paper, analyses were conducted on isotropic beams with rectangular and I-shaped cross-sections and the governing differential equations were solved via the Navier type closed-form solution. Instead, in Carrera et al. (2009), displacement unknowns were expanded by using N-order Lagrange polynomials (LE) which were defined on a set of sampling points belonging to the section. Several analyses were also conducted on a square section beam by adopting finite element procedure. Many studies have been devoted to evaluating the capabilities of the new refined elements. In Carrera et al. (2010), Carrera et al. analyzed the static behavior of a beam with an airfoil-like section under a bending load by using TE elements. They pointed out that the use of higher-order theories improves the flexibility feature of the finite element model and the accuracy of the displacement, stress and strain distributions over the cross-section. Beam formulation was employed to analyze the static behavior of thin-walled structures, bridge-like cross-sections (Carrera et al., 2012), furthermore, to present buckling and static analyses of laminated composite beams (Ibrahim et al., 2012; Catapano et al., 2011). With regard to the TE model, it has been found that the number of terms that have to be retained for each of the beam theories considered is closely related to the problem addressed. A comprehensive discussion of this issue is proposed by Carrera and Petrolo (2011). Dynamic analyses have also been dealt with in many works. For instance, in Carrera et al. (2011a), Petrolo et al. (2012) and (Carrera et al., submitted for publication) the dynamic characteristics of different beam sections and wing model are presented. Moreover, free-vibration investigations have been carried out on hollow cylindrical reinforced structures (Carrera et al., in press), laminated composite (Giunta et al., submitted for publication) and functionally graded beams (Giunta et al., 2011). In Carrera et al. (submitted for publication) several functions are tested to investigate the static behavior of compact, thin-walled and unconventional sections subjected to different load and boundary conditions. Many other papers in the literature report the features of CUF, but for a thorough and clear description it is recommended to refer to (Carrera et al., 2011b).

In this work, displacement components are defined by using trigonometric, exponential, hyperbolic and miscellaneous series. Symmetric and antisymmetric cross-ply laminated beams are considered. The results are reported in terms of displacements and stress and they are compared with those found in the literature or obtained by finite element models. For the sake of clarity, the results are preceded by a brief description of beam theory and finite element formulation.

2. Theories considered

A brief overview of the displacement models which have been implemented and compared in the present work is given in the following sections.

2.1. Classical theories

Linear distribution of the displacement u_y and a constant distributions of u_x and u_z across the cross-section (see Fig. 1) is assumed by classical beam theories. The displacement field above the beam cross-section is:

$$\begin{aligned} u_x &= u_{0x}(y) \\ u_y &= u_{0y}(y) + \theta(y)x + \phi(y)z \\ u_z &= u_{0z}(y) \end{aligned} \tag{1}$$

where u_{0x}, u_{0y}, u_{0z} are the displacements along the three directions; θ and ϕ are the rotations around z- and x-axis, respectively. The Euler–Bernoulli theory (Euler, 1744) introduces a further assumption to neglect the transverse shear deformations ε_{xy} and ε_{yz}. The related displacement field becomes:

$$\begin{aligned} u_x &= u_{0x}(y) \\ u_y &= u_{0y}(y) - u_{x,y}(y)x - u_{z,y}(y)z \\ u_z &= u_{0z}(y) \end{aligned} \tag{2}$$

However, the shear stress play an important role in various beam problems. By including the shear deformations ε_{xy} and ε_{yz}, the Eq. (1) represents the kinematic field of the Timoshenko theory (Timoshenko, 1921) which could also be written in the following form:

$$\begin{aligned} u_x &= u_{0x}(y) \\ u_y &= u_{0y}(y) + (\varepsilon_{xy} - u_{x,y})x + (\varepsilon_{yz} - u_{z,y})z \\ u_z &= u_{0z}(y) \end{aligned} \tag{3}$$

which is equivalent to Eq. (1) and the shear strains (ε_{xy}, ε_{yz}) and bending contributions ($u_{x,y}$, $u_{z,y}$) are separate.

Even though the Timoshenko model provides a constant distribution of shear deformation above the cross-section, it is not able to detect more complex deformations/stress state of the cross-section, such as the out- and in-plane deformations and the bending/torsion coupling.

2.2. Refined theories

Many attempts have been made to improve classical beam models. For instance, the warping functions (see Novozhilov (1961), Dufort et al. (2011)) were introduced to detect the cross-section deformation:

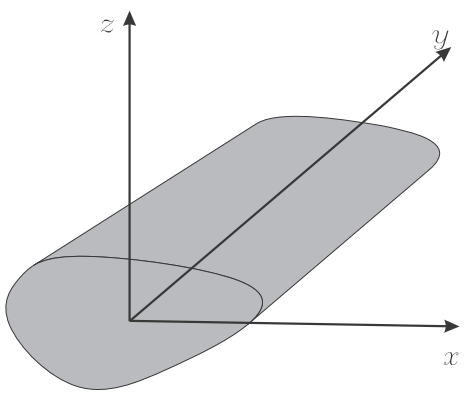

Fig. 1. Reference frame of the model.

$$\begin{aligned} u_x &= u_{0x}(y) \\ u_y &= u_{0y}(y) + f(x)(\varepsilon^o_{xy}) - u_{x,y}x + f(z)(\varepsilon^o_{yz}) - u_{z,y}z \\ u_z &= u_{0z}(y) \end{aligned} \tag{4}$$

where $f(x)$ and $f(z)$ are the warping functions and ε^o_{xy}, ε^o_{yz} are the transverse shear strains measured on the beam reference axis. So far, Eq. (4) neglect the in-plane axial strains ε_{xx} and ε_{zz}. Theories (2)–(4) are all based on hypotheses, which may be too restrictive.

To circumvent the problem, other higher-order theories have been derived such as Matsunaga's model (Matsunaga, 2002) in which the displacement components are expressed as follows:

$$\begin{aligned} u_x &= 0 \\ u_y &= z^n u_{y_n} \\ u_z &= z^n u_{z_n} \end{aligned} \tag{5}$$

where, according to the generalized Einstein notation, the subscripts and superscripts indicate summation.

However, for a complete removal of the inconsistencies we should assume the displacement field as an arbitrary expansion of generic functions (at least theoretically). Hence, we can write the displacements as:

$$\mathbf{u} = F_\tau(x,z)\mathbf{u}_\tau(y), \quad \tau = 1,2,\ldots,M \tag{6}$$

where u_τ is the displacement vector and M stands for the number of terms of the expansion. Since both the number of terms and the functions F_τ could depend on the features of the problems, they need to be chosen properly. Unfortunately, the major drawback of this method is the large number of related governing equations. The Carrera's Unified Formulation (CUF) represents a possible avenue to tackle this problem. In fact, the CUF offers a systematic procedure to obtain every kind of displacement theory, as showed in Carrera (2002, 2003b), Carrera and Petrolo (2011), Carrera et al. (2010, 2011a). This approach permits us to deal with any-order of beam theories without need of *ad hoc* implementations. A comprehensive introduction to CUF can be found in the book by Carrera et al. (Carrera et al., 2011b).

In line with Washizu (1975), in previous works, Eq. (6) has been employed by adopting a MacLaurin expansion that uses 2D polynomials $x^i z^j$ as base (i and j are positive integers). The capabilities of these functions have been assessed in the literature. For example, the second-order displacement field is:

$$\begin{aligned} u_x &= u_{x_1} + xu_{x_2} + zu_{x_3} + x^2u_{x_4} + xzu_{x_5} + z^2u_{x_6} \\ u_y &= u_{y_1} + xu_{y_2} + zu_{y_3} + x^2u_{y_4} + xzu_{y_5} + z^2u_{y_6} \\ u_z &= u_{z_1} + xu_{z_2} + zu_{z_3} + x^2u_{z_4} + xzu_{z_5} + z^2u_{z_6} \end{aligned} \tag{7}$$

while the third-order displacement field becomes:

$$\begin{aligned} u_x &= u_{x_1} + xu_{x_2} + zu_{x_3} + x^2u_{x_4} + xzu_{x_5} + z^2u_{x_6} + x^3u_{x_7} + x^2zu_{x_8} \\ &\quad + xz^2u_{x_9} + z^3u_{x_{10}} \\ u_y &= u_{y_1} + xu_{y_2} + zu_{y_3} + x^2u_{y_4} + xzu_{y_5} + z^2u_{y_6} + x^3u_{y_7} + x^2zu_{y_8} \\ &\quad + xz^2u_{y_9} + z^3u_{y_{10}} \\ u_z &= u_{z_1} + xu_{z_2} + zu_{z_3} + x^2u_{z_4} + xzu_{z_5} + z^2u_{z_6} + x^3u_{z_7} + x^2zu_{z_8} \\ &\quad + xz^2u_{z_9} + z^3u_{z_{10}} \end{aligned} \tag{8}$$

Eqs. (7) and (8) show two examples of refined displacement models. The classical models can be considered as a particular case of these expansions. If we compare the refined models with the one

reported in Eq. (1) it is clear that both have the constant terms, u_{x_1}, u_{y_1} and u_{z_1}. The coefficients of the linear terms in Eq. (1), $\theta(y)$ and $\phi(y)$, correspond to u_{y_2} and u_{y_3} in Eqs. (7) and (8). The terms over the linear one represent the warping of the section, higher the number of terms, more flexible is the cross-section.

A remarkable feature is that classical beam theories are obtainable as particular cases of Taylor expansions. It should be noted that classical theories require reduced material stiffness coefficients to contrast Poisson's locking. Unless otherwise specified, for classical and first-order models Poisson's locking is corrected according to Carrera and Giunta (Carrera et al., 2011b).

2.3. Advanced theories based on trigonometric and exponential expansions

Many attempts have been made in which the displacement fields have been obtained by using different functions. Since CUF makes it possible to deal with higher-order theories and it is invariant with respect to both any order N and any type of $F_\tau(x, z)$ function, it is simple to define new kinematic models (see Carrera et al., 2011b). For example, if we adopt a trigonometric series, the displacement components become:

$$\begin{aligned}
u_x &= \sin\left(\frac{\pi x}{a}\right)u_{x_1} + \cos\left(\frac{\pi x}{a}\right)u_{x_2} + \sin\left(\frac{\pi z}{b}\right)u_{x_3} + \cos\left(\frac{\pi z}{b}\right)u_{x_4} \\
&\quad + \sin\left(2\frac{\pi x}{a}\right)u_{x_5} + \dots \\
u_y &= \sin\left(\frac{\pi x}{a}\right)u_{y_1} + \sin\left(\frac{\pi x}{a}\right)u_{y_2} + \sin\left(\frac{\pi z}{b}\right)u_{y_3} + \cos\left(\frac{\pi z}{b}\right)u_{y_4} \\
&\quad + \sin\left(2\frac{\pi x}{a}\right)u_{y_5} + \dots \\
u_z &= \sin\left(\frac{\pi x}{a}\right)u_{z_1} + \sin\left(\frac{\pi x}{a}\right)u_{z_2} + \sin\left(\frac{\pi z}{b}\right)u_{z_3} + \cos\left(\frac{\pi z}{b}\right)u_{z_4} \\
&\quad + \sin\left(2\frac{\pi x}{a}\right)u_{z_5} + \dots
\end{aligned}$$

or by choosing an exponential expansion:

$$\begin{aligned}
u_x &= e^{\left(\frac{x}{a}\right)}u_{x_1} + e^{\left(\frac{z}{b}\right)}u_{x_2} + e^{\left(2\frac{x}{a}\right)}u_{x_3} + e^{\left(2\frac{z}{b}\right)}u_{x_4} + \dots \\
u_y &= e^{\left(\frac{x}{a}\right)}u_{y_1} + e^{\left(\frac{z}{b}\right)}u_{y_2} + e^{\left(2\frac{x}{a}\right)}u_{y_3} + e^{\left(2\frac{z}{b}\right)}u_{y_4} + \dots \\
u_z &= e^{\left(\frac{x}{a}\right)}u_{z_1} + e^{\left(\frac{z}{b}\right)}u_{z_2} + e^{\left(2\frac{x}{a}\right)}u_{z_3} + e^{\left(2\frac{z}{b}\right)}u_{z_4} + \dots
\end{aligned}$$

where a, b are the main cross-section dimensions.

2.4. Advanced zig-zag theories

Murakami (1986) introduced his function in the first order shear deformation theory with the purpose of reproducing the zig-zag form for the displacements of laminated plates. Due to the intrinsic anisotropy of multilayered structures, the first derivative of the displacement variables in the z-direction is discontinuous. The considered function is able to describe the aforementioned discontinuity (see Fig. 2). Since it is possible to use the zig-zag function in CUF framework, hereafter the theories which contain the term are identified with the exponent $_{zz}$. For example, $TE2^{zz}$:

$$\begin{aligned}
u_x &= u_{x_1} + xu_{x_2} + zu_{x_3} + x^2u_{x_4} + xzu_{x_5} + z^2u_{x_6} + (-1)^k\zeta_k u_{x_{7z}} \\
u_y &= u_{y_1} + xu_{y_2} + zu_{y_3} + x^2u_{y_4} + xzu_{y_5} + z^2u_{y_6} + (-1)^k\zeta_k u_{y_{7z}} \\
u_z &= u_{z_1} + xu_{z_2} + zu_{z_3} + x^2u_{z_4} + xzu_{z_5} + z^2u_{z_6} + (-1)^k\zeta_k u_{z_{7z}}
\end{aligned}$$

where $\zeta_k = 2z_k/h_k$ is a non-dimensional layer coordinate and h_k the thickness of the k-layer. The exponent k changes the sign of the zig-zag term in each layer.

2.5. Advanced theories based on miscellaneous expansions

To further improve the kinematic model, we can combine the different functions by obtaining miscellaneous expansions. One expansion is given below:

$$\begin{aligned}
u_x &= u_{x_1} + xu_{x_2} + zu_{x_3} + x^2u_{x_4} + xzu_{x_5} + z^2 + e^{\left(1\frac{x}{a}\right)}u_{x_6} + e^{\left(1\frac{z}{b}\right)}u_{x_7} \\
&\quad + \sin\left(3\frac{\pi x}{a}\right)u_{x_8} \\
u_y &= u_{y_1} + xu_{y_2} + zu_{y_3} + x^2u_{y_4} + xzu_{y_5} + z^2 + e^{1\left(\frac{x}{a}\right)}u_{y_6} + e^{\left(1\frac{z}{b}\right)}u_{y_7} \\
&\quad + \sin\left(3\frac{\pi x}{a}\right)u_{y_8} \\
u_z &= u_{z_1} + xu_{z_2} + zu_{z_3} + x^2u_{z_4} + xzu_{z_5} + z^2 + e^{\left(1\frac{x}{a}\right)}u_{z_6} + e^{\left(1\frac{z}{b}\right)}u_{z_7} \\
&\quad + \sin\left(3\frac{\pi x}{a}\right)u_{z_8}
\end{aligned}$$

Further cases will be directly described in the numerical discussion.

3. The FE formulation of various theories

A classical Finite Element technique is adopted with the purpose of easily dealing with arbitrary shaped cross-sections. The generalized displacement vector is given by:

$$\mathbf{u}_\tau(y) = N_i(y)\mathbf{q}_{\tau i} \tag{9}$$

where N_i are the shape functions and $\mathbf{q}_{\tau i}$ is the nodal displacement vector:

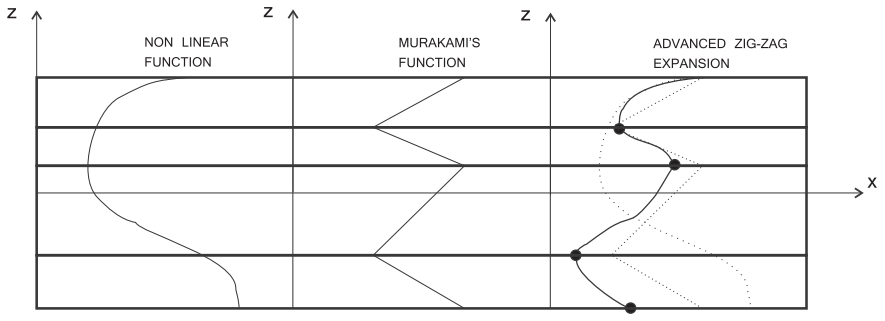

Fig. 2. Inclusion of the Murakami's function to higher order distribution.

$$\mathbf{q}_{\tau i} = \left\{ q_{u_{x_{\tau i}}} \quad q_{u_{y_{\tau i}}} \quad q_{u_{z_{\tau i}}} \right\}^T \tag{10}$$

For the sake of brevity, the shape functions are not listed here. They can be found in the literature, for instance in Bathe (1996). In this paper elements with 4 nodes (B4) are formulated using the Lagrange formulation, therefore a cubic approximation along the y axis is adopted. The functions are defined in the natural coordinates and transpose in the real coordinate in according with the iso-parametric formulation. The theory order of the beam model is related to the expansion on the cross-section and it is not correlated with the number of nodes per element along the y axis. In other words, these two parameters are totally free and not related to each other. The stiffness matrix of the elements and the external loadings, which are consistent with the model, are obtained via the Principle of Virtual Displacements:

$$\delta L_{\text{int}} = \int_V (\delta \varepsilon_p^T \boldsymbol{\sigma}_p + \delta \varepsilon_n^T \boldsymbol{\sigma}_n) \mathrm{d}V = \delta L_{\text{ext}} \tag{11}$$

Where L_{int} stands for the strain energy, L_{ext} is the work of external loadings and δ stands for virtual variation. The stress, $\boldsymbol{\sigma}$, and strain, ε, components are considered grouped as follows:

$$\begin{aligned} \boldsymbol{\sigma}_p &= \{ \sigma_{zz} \quad \sigma_{xx} \quad \sigma_{zx} \}^T, \quad \varepsilon_p = \{ \varepsilon_{zz} \quad \varepsilon_{xx} \quad \varepsilon_{zx} \}^T \\ \boldsymbol{\sigma}_n &= \{ \sigma_{zy} \quad \sigma_{xy} \quad \sigma_{yy} \}^T, \quad \varepsilon_n = \{ \varepsilon_{zy} \quad \varepsilon_{xy} \quad \varepsilon_{yy} \}^T \end{aligned} \tag{12}$$

The subscript "p" stands for terms lying on the cross-section, while "n" stands for terms lying on the other planes, which are orthogonal to the cross-section. The linear strain–displacement relations and the Hooke's law are, respectively:

$$\begin{aligned} \varepsilon_p &= \boldsymbol{D_p} \boldsymbol{u} \\ \varepsilon_n &= (\boldsymbol{D_{ny}} + \boldsymbol{D_{np}}) \boldsymbol{u} \end{aligned} \tag{13}$$

$$\begin{aligned} \boldsymbol{\sigma}_p &= \boldsymbol{C}_{pp} \varepsilon_p + \boldsymbol{C}_{pn} \varepsilon_n \\ \boldsymbol{\sigma}_n &= \boldsymbol{C}_{np} \varepsilon_p + \boldsymbol{C}_{nn} \varepsilon_n \end{aligned} \tag{14}$$

For an orthotropic material the matrices of the material coefficients are:

$$C_{pp}^k = \begin{bmatrix} \tilde{C}_{11}^k & \tilde{C}_{12}^k & \tilde{C}_{16}^k \\ \tilde{C}_{12}^k & \tilde{C}_{22}^k & \tilde{C}_{26}^k \\ \tilde{C}_{16}^k & \tilde{C}_{26}^k & \tilde{C}_{66}^k \end{bmatrix}, \quad C_{pn}^k = C_{np}^{T\,k} = \begin{bmatrix} 0 & 0 & \tilde{C}_{13}^k \\ 0 & 0 & \tilde{C}_{23}^k \\ 0 & 0 & \tilde{C}_{36}^k \end{bmatrix},$$
$$C_{nn}^k = \begin{bmatrix} \tilde{C}_{55}^k & \tilde{C}_{45}^k & 0 \\ \tilde{C}_{45}^k & \tilde{C}_{44}^k & 0 \\ 0 & 0 & \tilde{C}_{33} \end{bmatrix} \tag{15}$$

For the sake of brevity, the explicit forms of the coefficients of the matrices $\boldsymbol{C}$ are not included here, but they can be found in Tsai (1988) or Reddy (2004). The apex k refers to the layer, so each layer can have a different material. The virtual variation of the strain energy is rewritten using Eqs. (6), (9), (13) and (14) in a compact format it becomes:

$$\delta L_{\text{int}} = \delta q_{\tau i}^T \boldsymbol{K}^{ij\tau s} q_{si} \tag{16}$$

where $\boldsymbol{K}^{ij\tau s}$ is the stiffness matrix in the form of the fundamental nucleus. In a compact notation, it can be written as:

$$\begin{aligned} \boldsymbol{K}^{ij\tau s} = {} & I_l^{ij} \lhd (\boldsymbol{D}_{np}^T F_\tau \boldsymbol{I}) \left[\tilde{\boldsymbol{C}}_{np}^k (\boldsymbol{D}_p F_s \boldsymbol{I}) + \tilde{\boldsymbol{C}}_{nn}^k (\boldsymbol{D}_{np} F_s \boldsymbol{I}) \right] \\ & + (\boldsymbol{D}_p^T F_\tau \boldsymbol{I}) \left[\tilde{\boldsymbol{C}}_{pp}^k (\boldsymbol{D}_p F_s \boldsymbol{I}) + \tilde{\boldsymbol{C}}_{pn}^k (\boldsymbol{D}_{np} F_s \boldsymbol{I}) \right] \rhd_\Omega \\ & + I_l^{ij,y} \lhd \left[(\boldsymbol{D}_{np}^T F_\tau \boldsymbol{I}) \tilde{\boldsymbol{C}}_{nn}^k + (\boldsymbol{D}_p^T F_\tau \boldsymbol{I}) \tilde{\boldsymbol{C}}_{pn}^k \right] F_s \rhd_\Omega \boldsymbol{I}_{\Omega y} \\ & + I_l^{i,yj} \boldsymbol{I}_{\Omega y} \lhd F_\tau \left[\tilde{\boldsymbol{C}}_{np}^k (\boldsymbol{D}_p F_s \boldsymbol{I}) + \tilde{\boldsymbol{C}}_{nn}^k (\boldsymbol{D}_{np} F_s \boldsymbol{I}) \right] \rhd_\Omega \\ & + I_l^{i,yj,y} \boldsymbol{I}_{\Omega\, y} \lhd F_\tau \tilde{\boldsymbol{C}}_{nn}^k F_s \rhd_\Omega \boldsymbol{I}_{\Omega\, y} \end{aligned} \tag{17}$$

Where:

$$\boldsymbol{I}_{\Omega y} = \begin{bmatrix} 0 & 0 & 1 \\ 1 & 0 & 0 \\ 0 & 1 & 0 \end{bmatrix} \quad \lhd \ldots \rhd_\Omega = \int_\Omega \ldots \mathrm{d}\Omega \tag{18}$$

$$\left(I_l^{ij}, I_l^{ij,y}, I_l^{i,yj}, I_l^{i,yj,y} \right) = \int_l \left(N_i N_j, N_i N_{j,y}, N_{i,y} N_j, N_{i,y} N_{j,y} \right) \mathrm{d}y \tag{19}$$

The apex k indicates the layer so the material is considered not constant in the integral over the cross-section Ω (see. Eq. (18)). This allows to investigate composite structure and non-homogenous sections. The work of the external forces, δL_{ext} can be expressed as:

$$\begin{aligned} \delta L_{\text{ext}} &= \int_V \left(\tilde{F} \delta u \right) \mathrm{d}V \\ &= \delta \mathbf{q}_{\tau i}^T \int_V N_i(y) F_\tau(x,z) \mathrm{d}V \\ &= \delta \mathbf{q}_{\tau i}^T \mathbf{P}^{\tau i} \end{aligned} \tag{20}$$

where $\tilde{F}$ is the generic load and $[\mathbf{P}^{\tau i}]$ is the vector of the nodal forces.

The global matrices can be indicate as $\tilde{\mathbf{K}}$ for the stiffness matrix, $\tilde{\mathbf{F}}$ for the vector of the nodal forces and $\mathbf{q}$ for the unknowns. The problem to solve, represented in Eq. (11), can be written in the following terms:

$$\begin{aligned} \delta \mathbf{q}^T \tilde{\mathbf{K}} q &= \delta \mathbf{q}^T \tilde{\mathbf{P}} \\ \tilde{\mathbf{K}} q &= \tilde{\mathbf{P}} \end{aligned} \tag{21}$$

It should be noted that no assumptions on the approximation order have been made. It is therefore possible to obtain refined beam models without changing the formal expression of the nucleus components. This is the key point of CUF which allows the implementation of any-order one-dimensional theories with only nine FORTRAN statements.

4. Numerical analyses and discussion

4.1. Nomenclature used to denote various expansions

This section aims to assess the accuracy of the various theories discussed in Section 2. The expansions considered are summarized in Table 1 by adopting some nomenclatures. In order to understand their meaning, we may refer to the following short expressions:

- Functions with single trigonometric term:

$$sx = \sin\left(m\frac{\pi x}{a}\right) \quad cx = \cos\left(m\frac{\pi x}{a}\right) \quad sz = \sin\left(n\frac{\pi z}{b}\right) \quad cz = \cos\left(n\frac{\pi z}{b}\right)$$

$$sd = \sin\left(mn\frac{\pi xz}{ab}\right) \quad cd = \cos\left(mn\frac{\pi xz}{ab}\right)$$

Table 1
Expansions.

	$\overline{1}$	$\overline{2}$	$\overline{3}$	$\overline{4}$	$\overline{5}$	6	7	$\overline{8}$	$\overline{9}$	$\overline{10}$	11	12
cost	✓	✓	✓	✓	✓			✓	✓	✓	✓	✓
sx	✓		✓	✓	✓				✓		✓	✓
cx		✓	✓	✓	✓				✓		✓	✓
sz	✓		✓	✓	✓				✓		✓	✓
cz		✓	✓	✓	✓				✓		✓	✓
sd				✓								✓
cd				✓								✓
cc					✓	✓						
cs					✓	✓						
sc					✓	✓						
ss					✓	✓						
cscs							✓					
expx								✓	✓			
expz								✓	✓			
shx										✓	✓	✓
chx										✓	✓	✓
shz										✓	✓	✓
chz										✓	✓	✓
TE	✓	✓	✓	✓	✓			✓	✓	✓	✓	✓

($\bar{\bullet}$): $m = n$.

- Functions with two trigonometric terms:

$$cc = \cos\left(m\frac{\pi x}{a}\right)\cos\left(n\frac{\pi z}{b}\right) \quad cs = \cos\left(m\frac{\pi x}{a}\right)\sin\left(n\frac{\pi z}{b}\right)$$
$$sc = \sin\left(m\frac{\pi x}{a}\right)\cos\left(n\frac{\pi z}{b}\right) \quad ss = \sin\left(m\frac{\pi x}{a}\right)\sin\left(n\frac{\pi z}{b}\right)$$

- Functions with three/four trigonometric factors:

$$csc = \cos\left(l\frac{\pi x}{a}\right)\sin\left(m\frac{\pi x}{a}\right)\cos\left(n\frac{\pi z}{b}\right)$$
$$cscs = \cos\left(l\frac{\pi x}{a}\right)\sin\left(m\frac{\pi x}{a}\right)\cos\left(n\frac{\pi z}{b}\right)\sin\left(p\frac{\pi z}{b}\right)$$

- Hyperbolic functions:

$$chx = \cosh(mx) \quad shx = \sinh(mx) \quad chz = \cosh(nz) \quad shz = \sinh(nz)$$

- Exponential functions:

$$expx = e^{(mx)} \quad expz = e^{(nz)}$$

where l, m, n, p are the numbers of waves along the x and z-direction. For instance, the first component of the displacement vector related to $E10$ with 13 terms of Table 1 corresponds to the following expansion:

$$u_x = F_\tau u_{x\tau} \tag{22}$$

Table 2
Effect of the number (n_e) of elements B4 on $-u_z$ ($\times 10^{-3}[m]$). Loading case: bending.

N	$n_e = 1$	$n_e = 5$	$n_e = 10$	$n_e = 30$
CBT	1.3703	1.3703	1.3703	1.3703
FOBT	1.3704	1.3704	1.3704	1.3704
TE_1	1.3704	1.3704	1.3704	1.3704
TE_3	1.2728	1.3442	1.3534	1.3597
TE_5	1.2840	1.3541	1.3627	1.3684
Ref. Eq. (23) = 1.3698				

CBT stands for Classical beam theory. *FOBT* stands for First-order beam theory.

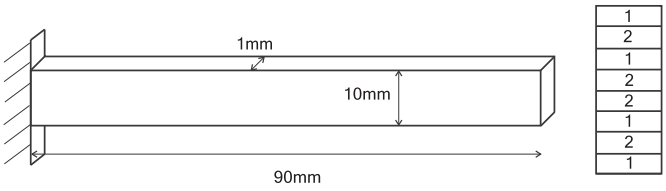

Fig. 3. The eight-layer laminated beam.

where, in addition to the constant term, the functions F_τ become:

$$F_\tau = \cosh(mx) \quad m = 2,3,4$$
$$F_\tau = \sinh(mx) \quad m = 5,6,7$$
$$F_\tau = \cosh(mz) \quad m = 8,9,10$$
$$F_\tau = \sinh(mz) \quad m = 11,12,13$$

If Taylor's polynomials have been added to displacement fields, their order has been specified by the subscript. In the case that a complete expansion is used, the subscript is *'higher order polynomial'-c*, while in contrast, if only some polynomials are employed, their orders are explicitly reported and divided by a comma. For the sake of clarity, in the following are presented the examples related to the two mentioned options for the first component of the displacement field 22:

- $E3_{2\ -\ c}$ with 14 terms:

$$\begin{aligned} u_x = {} & cost\, u_{x_1} + \sin\left(\frac{\pi x}{a}\right)u_{x_2} + \cos\left(\frac{\pi x}{a}\right)u_{x_3} + \sin\left(\frac{\pi z}{b}\right)u_{x_4} \\ & + \cos\left(\frac{\pi z}{b}\right)u_{x_5} + \sin\left(2\frac{\pi x}{a}\right)u_{x_6} + \cos\left(2\frac{\pi x}{a}\right)u_{x_7} \\ & + \sin\left(2\frac{\pi z}{b}\right)u_{x_8} + \cos\left(2\frac{\pi z}{b}\right)u_{x_9} + xu_{x_{10}} + zu_{x_{11}} \\ & + x^2u_{x_{12}} + xzu_{x_{13}} + z^2u_{x_{14}} \end{aligned}$$

Table 3
Deflections and stresses of the laminated beam.

	N	$-u_z \times 10^{-2}$	$-\sigma_{yy}$	DOFs
Surana and Nguyen (1990)		3.031	720	
Davalos and KimBarbero (1994)		3.029	700	
Xiaoshan Lin (2011)		3.060	750	
Vo and Thai (2012)		3.024		
CBT		2.629	730	279
FOBT		2.988	730	279
TE_1	zz	2.992	730	279
		2.992	730	372
TE_2	zz	2.985	730	558
		2.986	730	651
TE_3	zz	3.032	729	930
		3.033	729	1023
TE_9	zz	3.039	661	5115
		3.040	661	5208
$E1$	5	2.603	730	1023
	9	2.603	731	1767
	5_3	3.035	730	1860
$E2$	9	0.364	0.0	1767
$E3$	5	2.876	730	1953
	5_2	3.038	730	2418
$E4$	5	2.882	750	2883
	5_2	3.038	730	3348
$E5$	3_1	3.063	724	2511
$E6$	3	3.017	849	4557
$E7$	2	2.861	845	4557
$E8$	6_2	3.034	715	1674
	8_2	3.034	733	2046
$E9$	3_2	3.037	725	2418
$E10$	4_2	3.035	728	2046
	7	2.875	732	2697
$E11$	3_2	3.039	726	2790
$E12$	5	3.038	724	3255

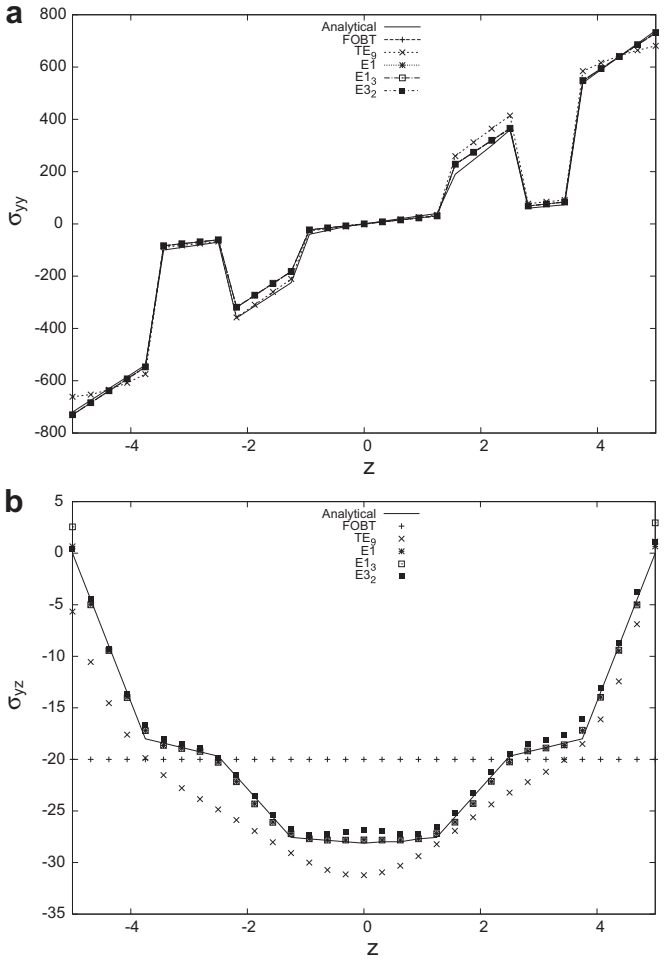

Fig. 4. Distribution of stresses $\overline{\sigma}_{yy}$ and $\overline{\sigma}_{yz}$ through-the-thickness at mid-span of the laminated cantilever beam ($L/h = 9$). (a) $-\overline{\sigma}_{yy}$, (b) $-\overline{\sigma}_{yz}$.

- $E3_{1,3}$ with 15 terms:

$$
\begin{aligned}
u_x = {} & \cos t\, u_{x_1} + \sin\left(\frac{\pi x}{a}\right) u_{x_2} + \cos\left(\frac{\pi x}{a}\right) u_{x_3} + \sin\left(\frac{\pi z}{b}\right) u_{x_4} \\
& + \cos\left(\frac{\pi z}{b}\right) u_{x_5} + \sin\left(2\frac{\pi x}{a}\right) u_{x_6} + \cos\left(2\frac{\pi x}{a}\right) u_{x_7} \\
& + \sin\left(2\frac{\pi z}{b}\right) u_{x_8} + \cos\left(2\frac{\pi z}{b}\right) u_{x_9} + x u_{x_{10}} + z u_{x_{11}} \\
& + x^3 u_{x_{12}} + x^2 z u_{x_{13}} + x z^2 u_{x_{14}} + z^3 u_{x_{15}}
\end{aligned}
$$

Table 4
Reference solutions related to symmetric beams under uniformly distributed load and for various boundary conditions.

Theory	*Ref.*	*C–F*			*S–S*		
		L/h			*L/h*		
		5	10	20	5	10	20
0/90/0							
CBT	Khdeir et al. (1997a)	2.198	2.198	2.198	0.646	0.646	0.646
	Vo and Thai (2012)	2.203	2.203	2.203	0.648	0.648	0.648
FOBT	Khdeir et al. (1997a)	6.698	3.323	–	2.146	1.021	–
	Vo and Thai (2012)	6.703	3.328	2.485	2.148	1.023	0.742
HOBT	Khdeir et al. (1997a)	6.824	3.455	–	2.412	1.096	–
	Vo and Thai (2012)	6.830	3.461	2.530	2.414	1.098	0.761
SSBT	Vo and Thai (2012)	6.842	3.478	2.536	2.444	1.108	0.764

HOBT stands for Higher-order beam theory.
SSBT stands for Sinusoidal shear beam theory.

Table 5
Reference solutions related to antisymmetric beams under uniformly distributed load and for various boundary conditions.

Theory	Ref.	*C–F*			*S–S*		
		L/h			*L/h*		
		5	10	20	5	10	20
0/90							
CBT	Khdeir et al. (1997a))	11.293	11.293	11.293	3.322	3.322	3.322
	Vo and Thai (2012)	11.319	11.319	11.319	3.329	3.329	3.329
FOBT	Khdeir et al. (1997a)	16.436	12.579	–	5.036	3.750	–
	Vo and Thai (2012)	16.461	12.604	11.640	5.043	3.757	3.436
HOBT	Khdeir et al. (1997a)	15.279	12.343	–	4.777	3.688	–
	Vo and Thai (2012)	15.305	12.369	11.588	4.785	3.696	3.421
SSBT	Vo and Thai (2012)	15.173	12.340	11.582	4.749	3.687	3.419

HOBT stands for Higher-order beam theory.
SSBT stands for Sinusoidal shear beam theory.

4.2. Convergence study

Before the finite element analysis of composite beams is reported, it is useful to consider the results from the convergence study. A cantilever beam with aspect-ratio assumed to be equal to 100 is considered. The material is aluminum with the Young Modulus and the Poisson ratio equal to 73 GPa and 0.34, respectively. The cross-section is square and a concentrated load ($F_z = -25\ N$) is applied on the free tip. The reference solution is provided by the following formula:

$$u_z(y = L) = \frac{F_z L^3}{3EI} \tag{23}$$

Table 6
Non-dimensional mid-span displacements of a symmetric cross-ply beam under a uniformly distributed load.

	N	*C–F*			*S–S*			DOFs
		L/h			*L/h*			
		5	10	20	5	10	20	
CBT		2.203	2.203	2.203	0.649	0.649	0.649	198
FOBT		5.946	3.140	2.438	1.898	0.961	0.727	198
TE_1	*zz*	5.946	3.140	2.438	1.898	0.961	0.727	198
		7.337	3.602	2.569	2.534	1.478	0.776	264
TE_2	*zz*	5.936	3.137	2.435	1.886	0.960	0.726	396
		7.322	3.597	2.566	2.520	1.145	0.775	462
TE_3	*zz*	7.146	3.513	2.539	2.415	1.106	0.764	660
		7.512	3.660	2.584	2.606	1.171	0.781	726
TE_6	*zz*	7.275	3.575	2.560	2.484	1.134	0.772	1848
		7.580	3.670	2.586	2.610	1.171	0.781	1914
*E*1	5	7.449	3.616	2.562	2.564	1.152	0.774	726
	5^{zz}	7.573	3.658	2.574	2.619	1.169	0.778	792
*E*3	5	7.453	3.624	2.571	2.554	1.153	0.776	1386
	5^{zz}	7.577	3.666	2.582	2.610	1.170	0.780	1452
*E*4	5	7.457	3.628	2.574	2.554	1.154	0.777	2046
	5^{zz}	7.581	3.670	2.586	2.610	1.171	0.782	2112
*E*5	4	7.454	3.628	2.573	2.556	1.154	0.777	2178
	4^{zz}	7.579	3.668	2.584	2.603	1.171	0.781	2244
*E*6	2	7.259	3.453	2.080	2.077	0.782	0.390	1650
	3	7.275	3.562	2.515	2.079	0.784	0.398	3234
	3^{zz}	7.567	3.662	2.565	2.461	0.893	0.428	3300
*E*7	2	7.455	3.629	2.575	2.548	1.153	0.776	3234
	2^{zz}	7.580	3.669	2.586	2.605	1.170	0.780	3300
*E*8	7	7.348	3.596	2.563	2.104	0.791	0.402	990
	7^{zz}	7.576	3.666	2.582	2.180	0.893	0.428	1056
	7_1^{zz}	7.578	3.666	2.582	2.611	1.156	0.775	1188
*E*9	2	7.294	3.580	2.559	2.496	1.137	0.770	858
	2^{zz}	7.575	3.666	2.582	2.606	1.166	0.779	924
*E*10	3	7.264	3.568	2.555	2.479	1.132	0.771	858
	3^{zz}	7.576	3.666	2.582	2.610	1.170	0.781	924
*E*11	3	7.455	3.625	2.571	2.555	1.154	0.776	1650
	3^{zz}	7.579	3.666	2.582	2.610	1.170	0.781	1716
*E*12	2	7.431	3.621	2.572	2.544	1.152	0.777	1386
	2^{zz}	7.580	3.669	2.586	2.610	1.171	0.782	1452

Table 7
Non-dimensional mid-span displacements of an antisymmetric cross-ply beam under a uniformly distributed load.

	N	C–F			S–S			DOFs
		L/h			L/h			
		5	10	20	5	10	20	
CBT		11.330	11.339	11.344	3.337	3.340	3.341	198
FOBT		15.606	12.410	11.612	4.764	3.697	3.430	198
TE_1	zz	15.559	12.409	11.612	4.757	3.696	3.430	198
		15.661	12.457	11.626	4.805	3.714	3.435	264
TE_2	zz	15.643	12.401	11.586	4.792	3.704	3.428	396
		15.683	12.414	11.590	4.810	3.709	3.430	462
TE_5	zz	16.209	12.565	11.635	5.008	3.762	3.445	1386
		16.255	12.576	11.638	5.022	3.765	3.446	1452
TE_6	zz	16.215	12.566	11.636	5.009	3.762	3.445	1848
		16.264	12.580	11.640	5.027	3.766	3.446	1914
E1	5	15.840	12.326	11.440	4.898	3.689	3.386	726
	5^{zz}	16.073	12.483	11.569	4.980	3.741	3.426	792
E3	5	16.247	12.567	11.627	5.007	3.761	3.443	1386
	5^{zz}	16.275	12.573	11.629	5.028	3.764	3.443	1452
E4	5	16.250	12.571	11.631	5.001	3.762	3.444	2046
	5^{zz}	16.278	12.577	11.633	5.027	3.766	3.445	2112
E5	4	16.227	12.560	11.609	5.000	3.760	3.441	2178
	4^{zz}	16.271	12.573	11.612	5.026	3.765	3.443	2244
E6	3	16.201	12.440	11.110	3.229	1.827	1.455	3234
	3^{zz}	16.261	12.447	11.113	3.651	2.174	1.676	3300
E7	2	16.214	12.560	11.610	4.945	3.728	3.404	3234
	2^{zz}	16.261	12.572	11.614	4.975	3.735	3.407	3300
E8	7	16.222	12.560	11.624	3.232	1.827	1.720	990
	7^{zz}	16.260	12.570	11.629	3.656	2.179	1.721	1056
	7^{zz}_{1c}	16.264	12.571	11.629	5.007	3.761	3.442	1188
E9	2	16.215	12.558	11.625	4.946	3.726	2.777	858
	2^{zz}	16.256	12.570	11.628	4.975	3.734	2.871	924
E10	3	16.204	12.554	11.624	4.988	3.756	3.441	858
	3^{zz}	16.253	12.568	11.628	5.019	3.762	3.443	924
E11	3	16.241	12.567	11.626	5.006	3.760	3.443	1650
	3^{zz}	16.274	12.574	11.629	5.027	3.765	3.443	1716
E12	2	16.229	12.565	11.630	4.999	3.760	3.443	1386
	2^{zz}	16.273	12.577	11.633	5.025	3.765	3.444	1452

Table 8
Non-dimensional mid-span displacements and stresses of a symmetric cross-ply beam under a sinusoidal load. $L/h = 4$.

	N	$-u_z$	$\overline{\sigma}^{-}_{yy}$	$-\overline{\sigma}_{yz}$	DOFs
Pagano (1970)		2.8899	18.8	1.4318	
Vidal and Polit (2011)		2.8027	19.5	1.4202	
CBT		0.5114	10.0716	0.6687	198
FOBT		2.0904	10.0716	0.6339	198
TE_1	zz	2.0904	10.0716	0.6339	198
		2.7980	16.1831	1.4366	264
TE_2	zz	2.0693	10.4532	0.6295	396
		2.7774	16.6156	1.4357	462
TE_5	zz	2.7407	18.4559	1.2881	1386
		2.8857	19.1293	1.4115	1492
TE_6	zz	2.7421	18.5360	1.2894	1848
		2.8865	19.2155	1.4167	1914
E1	5	2.8448	18.1028	1.6170	726
	5^{zz}	2.9058	18.3784	1.4238	792
E3	4	2.8263	18.9183	1.5917	1122
	4^{zz}	2.8884	19.1943	1.4283	1188
E7	2	2.8164	18.7619	1.3487	3234
	2^{zz}	2.8806	19.0437	1.4428	3300
E8	7	2.4110	14.9279	0.8114	990
	7^{zz}	2.8026	17.6943	1.6698	1056
	7^{zz}_{1c}	2.8724	19.0909	1.4460	1188
E9	3	2.8218	19.0048	1.3986	1254
	3^{zz}	2.8819	19.3168	1.3679	1320
E10	4	2.8019	18.9997	1.4843	1122
	4^{zz}	2.8815	19.3500	1.4123	1320

Table 9
Non-dimensional mid-span displacements and stresses of an anti-symmetric cross-ply beam under a sinusoidal load. $L/h = 4$.

	N	$\overline{u}_z$	$-\overline{\sigma}^{-}_{yy} \times 10$	$\overline{\sigma}^{+}_{yy}$	$-\overline{\sigma}_{yz}$	DOFs
Pagano (1970)		4.6952	3.0028	3.8358	2.7061	
Vidal and Polit (2011)		4.5438	3.1800	–	2.8430	
CBT		2.6226	2.7876	3.0261	2.2585	198
FOBT		4.4270	2.7876	3.0261	1.8118	198
TE_1	zz	4.4512	2.7887	3.0261	1.7845	198
		4.5177	2.7968	3.2309	2.0217	264
TE_2	zz	4.4048	2.5369	3.5509	1.9578	396
		4.4219	2.6930	3.3824	2.0058	462
TE_5	zz	4.6589	2.9932	3.9365	2.5884	1386
		4.6789	2.8497	4.2537	2.6584	1452
TE_6	zz	4.6612	2.9776	3.9721	2.5800	1848
		4.6844	2.7684	4.4180	2.7092	1914
E1	5	4.5570	3.1109	3.3842	2.3958	726
	5^{zz}	4.6294	3.1455	3.5417	2.5820	792
E3	4	4.6499	2.9837	3.9441	2.6310	1122
	4^{zz}	4.6831	2.7092	4.5567	2.6852	1188
E7	2	4.6381	3.1175	3.6214	1.6603	3234
	2^{zz}	4.6767	3.1270	3.6388	1.8399	3300
E8	7	3.4067	2.0574	2.4455	2.3429	990
	7^{zz}	3.7251	2.4091	2.6545	1.6803	1056
	7^{zz}_{2c}	4.6604	2.7904	4.4441	2.1423	1386
E9	3	4.6541	3.0073	4.0071	2.6158	1254
	3^{zz}	4.6850	2.8135	4.4383	2.6993	1320
E10	4	4.6477	2.9499	4.0314	2.5813	1122
	4^{zz}	4.6830	2.7325	4.4921	2.6553	1320

Table 2 gives the results obtained using a variety of expansions. We can note that a higher number of elements (n_e) enhances the flexibility of the structure and the convergency strictly depends on both the order and the type of the approximations.

4.3. Analysis of an eight-layer composite beam

In the first case, a cantilever beam made up of eight orthotropic layers is considered. The geometric features and the symmetric stacking sequence of the structure are shown in Fig. 3. The elastic modulus in the transversal direction, the shear modulus, the and the Poisson's ratio of the two materials are equal and they are assumed to be 1 GPa, 0.5 GPa and 0.25, respectively. In contrast, the

Table 10
Non-dimensional displacements and stresses of a symmetric cross-ply beam under a uniform distributed load. σ_{yy} at ($b/2$; 0; −0.367 h) and σ_{zz} at ($b/2$; $L/2$; $h/2$). $L/h = 4$.

Nastran	N	$-\overline{u}_z$	$-\overline{\sigma}^{-}_{yy}$	$-\overline{\sigma}^{+}_{zz}$	DOFs	t/t_{CBT}
		17.9754	30.5844	1.0278	103920	
CBT		6.2245	36.5184	0.0000	198	1
FOBT		14.0223	36.5184	0.0000	198	1
TE_1	zz	14.0224	36.5184	0.4958	198	4
		17.3328	38.0646	0.4475	264	6
TE_2	zz	14.0154	36.3298	0.9368	396	13
		17.3060	37.8849	1.0556	462	16
TE_3	zz	16.7647	28.3861	1.0439	660	33
		17.7591	31.1710	1.0203	726	40
TE6	zz	17.1384	25.2949	0.9950	1848	271
		17.8371	27.3629	1.0323	1914	273
E1	5	17.5913	31.0081	0.4519	726	55
	5^{zz}	17.8900	29.7549	0.4527	792	63
E3	4	17.5344	29.1559	0.9490	1386	148
	4^{zz}	17.8306	26.9953	0.9482	1452	161
E8	7	17.3165	26.9024	1.0022	990	76
	7^{zz}	17.8317	26.3964	0.9753	1056	86
E10	4	17.4569	32.4646	0.9740	1122	100
	4^{zz}	17.8330	29.2696	0.9614	1188	122
E11	22	16.9478	29.8585	2.1963	1452	170
	$2^{zz}{}_2$	17.8294	29.0429	0.9644	1518	176

Table 11
Non-dimensional displacements and stresses of an antisymmetric cross-ply beam under a uniform distributed load. σ_{yy} at ($b/2$; 0; −0.328 h) and σ_{zz} at ($b/2$; $L/2$; $h/2$). $L/h = 4$.

Nastran	N	$\overline{u}_z$	$\overline{\sigma}_{yy}$	$-\overline{\sigma}^{+}_{yy}$	$-\overline{\sigma}^{+}_{zz}$	DOFs
		43.0937	36.1128	11.4270	1.0239	198300
CBT		31.9645	50.0290	11.4394	0.0000	198
FOBT		40.8757	50.0290	11.4394	0.0000	198
TE_1	*zz*	40.8609	50.0290	11.4394	0.3887	198
		41.2077	48.2077	13.0898	0.6001	264
TE_2	*zz*	40.9202	50.3749	13.2647	0.9811	396
		41.0123	48.3814	13.6445	0.9270	462
TE_3	*zz*	41.6311	36.7505	12.8075	1.1380	660
		41.6610	39.2040	11.2977	1.0460	726
TE_6	*zz*	42.1602	34.4559	11.1822	1.0487	1848
		42.2641	32.3570	11.1140	1.0125	1914
*E*1	5	41.0117	38.5647	12.0483	0.1629	726
	5^{zz}	41.8772	37.4122	13.2317	0.5258	792
*E*3	5	42.2615	38.2760	12.0058	1.0072	1386
	5^{zz}	42.3180	39.4730	11.8947	0.9835	1452
*E*7	2	42.1627	33.0495	11.4730	1.0055	3234
	2^{zz}	42.2647	32.7768	11.3875	1.0231	2450
*E*8	7	42.2088	33.3488	11.8175	1.0144	990
	7^{zz}	42.2872	31.6294	11.8706	1.0033	1056
*E*10	4	42.2152	37.1428	11.5646	0.9343	1122
	4^{zz}	42.3058	39.8400	11.5813	0.9668	1188

Young Modulus of material labeled with the number 1 is 30 GPa whereas that related to the second one is 5 GPa. In order to ensure the convergence, ten finite elements are used to model the structure along the *y-axis*. The structure is loaded at the tip by a concentrated load of $F_z = -0.2$ *N*. The results are presented in numerical and graphical form. In Table 3 the maximum deflections and the longitudinal stresses computed with different displacement theories are compared with those found in literature (Surana and Nguyen, 1990; Davalos and KimBarbero, 1994; Xiaoshan Lin, 2011; Vo and Thai, 2012) whereas Fig. 4 shows the distributions of σ_{yy} and σ_{yz} at mid-span for a variety of expansions. These distributions are compared with the analytical solutions derived by theory of elasticity presented in Lekhniskii et al. (1968). It can be seen that the results provided by *TE*, *E*6 and *E*12 expansions are in strong agreement with reference solutions both in term of displacements and normal stresses, while in contrast, the remaining trigonometric (especially *E*2), exponential and hyperbolic displacement theories underestimate, generally, the deflection. On the other hand, if we consider the distribution of the shear stress, σ_{yz} (see Fig. 4), the best solution is furnished by *E*1, in which the sinusoidal function is employed. The miscellaneous expansions are able to combine the features of the other expressions and, in fact, when the Taylor's polynomials are added to the sinusoidal function, the results are very close to the reference solutions (see $E1_3$, $E3_2$, $E8_2$). In the case in point, the zig-zag function does not strongly affect the solutions.

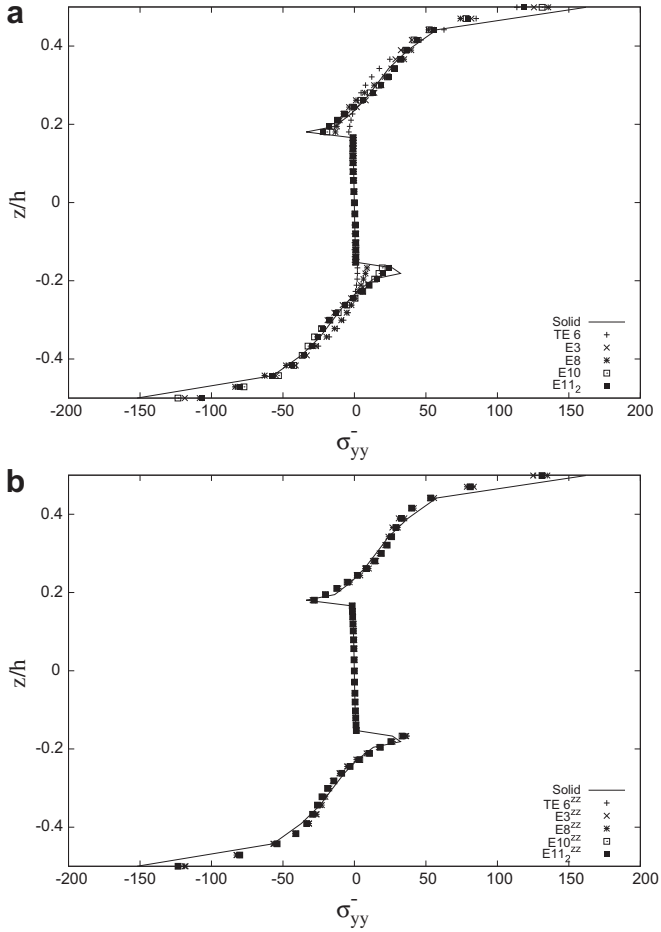

Fig. 5. Distribution of stresses $\overline{\sigma}_{yy}$ through-the-thickness of a symmetric cantilever beam ($L/h = 4$). (a) $-\overline{\sigma}_{yy}$, (b) $-\overline{\sigma}_{yy}$.

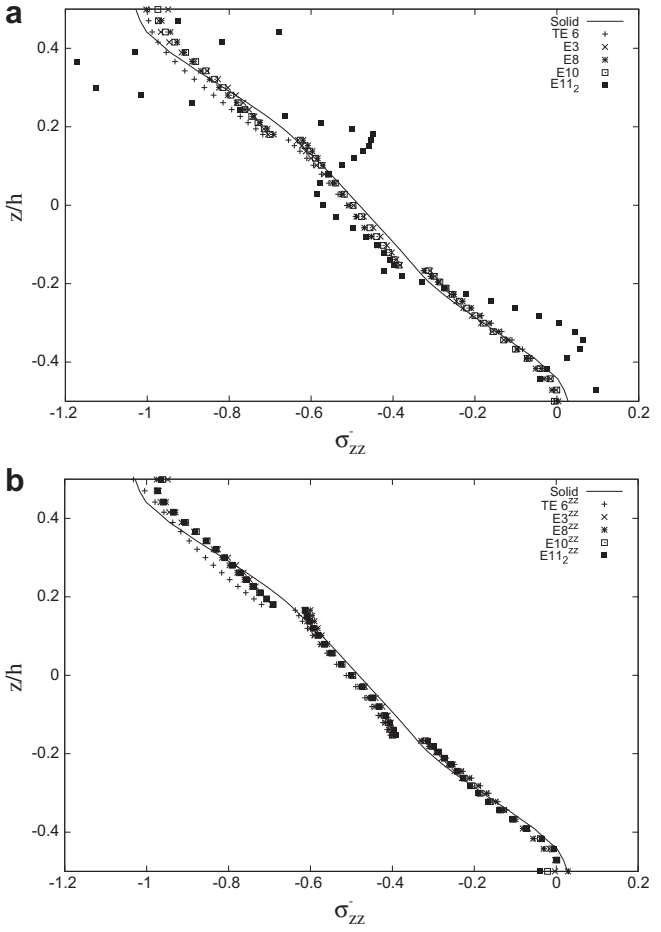

Fig. 6. Distribution of stresses $\overline{\sigma}_{zz}$ through-the-thickness of a symmetric cantilever beam ($L/h = 4$). (a) $-\overline{\sigma}_{zz}$, (b) $-\overline{\sigma}_{zz}$.

4.4. Symmetric and antisymmetric cross-ply laminated beams

The following section aims to present the results obtained for symmetric $(0°/90°/0°)$ and antisymmetric $(0°/90°)$ cross-ply laminated beams constituted by orthotropic material. All laminae are assumed to be of the same thickness and, if not otherwise declared, the dimensionless material properties adopted are:

$$E_A/E_T = 25 \quad G_{AT}/G_{TT} = 2.5 \quad \nu_{AT} = \nu_{TT} = 0.25$$

where A refers to the fiber direction and T refers to the normal direction.

For convenience, the results are presented in non-dimensional form:

$$\overline{u}_z = 100\frac{bh^3E_T}{q_0L^4}u_z, \quad \overline{\sigma}_{ij} = \frac{\sigma_{ij}}{q_0}, \quad \text{with} \quad i,j = x,y,z$$

where L is the length of the beam, b and h the dimensions of the rectangular cross-section and q_0 the intensity of the load. To model the structure seven finite elements are used.

In the first case, the load is assumed to be uniformly distributed and beams with clamped–free (C–F) and supported–supported (S–S) boundary conditions are considered. In Tables 4 and 5 the reference solutions are listed for several values of aspect-ratio (L/h). Tables 6 and 7 present the deflections computed with the various theories. As can be seen, the classical theories (*CBT* and *FOBT*) are not suitable for analyzing the static behavior of laminated beams, especially when the aspect-ratio decreases. Significant improvements are introduced by Taylor polynomials. For example for the symmetric beam, the third-order expansion yields greater displacement values than those of the reference solutions for all values of aspect-ratios and for the two boundary conditions. On the other hand, it is interesting to note that, by using other functions, the flexibility of the structure is further enhanced. The trigonometric and hyperbolic functions (see $E1$, $E3$, $E9$, $E10$, $E11$ and $E12$) are especially suitable for these kinds of problems. The expansion $E8$ represents a particular case, in fact for the C–F condition, the results agree very well with the reference solutions, while in contrast, for the supported boundaries the results become unacceptable. However, if Taylor polynomials are combined with the exponential function the results are very similar to the reference solutions. Furthermore, it has to be noted that the zig-zag function improves the solution markedly for all various expansions. For instance, by considering the first-order Taylor polynomial, with the zig-zag function the deflection value increases by about 20% for the symmetric beam.

In the second analysis, the aspect-ratio is fixed and it is assumed to be equal to 4. The symmetric and antisymmetric beams are simply supported and they are subjected to a sinusoidal load ($q = q_0 \sin \pi y/L$). The mid-span deflection and the normal (at $(b/2; L/2; \pm h/2)$) and transverse shear (at $(b/2; 0; -h/4)$) stresses presented in Tables 8 and 9 are compared with the solutions provided by

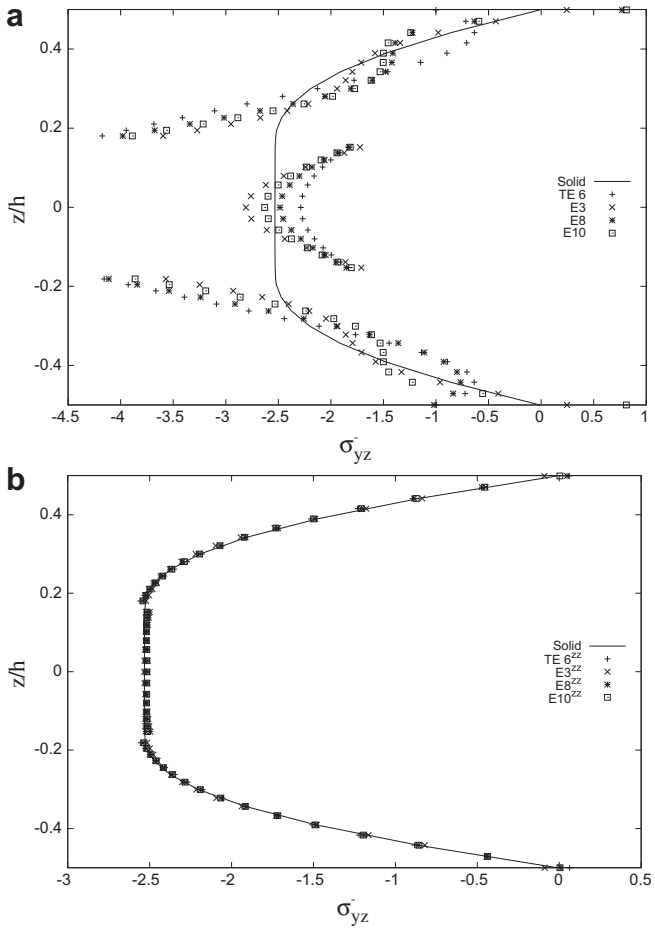

Fig. 7. Distribution of stresses $\overline{\sigma}_{yz}$ through-the-thickness of a symmetric cantilever beam $(L/h = 4)$. (a) – $\overline{\sigma}_{yz}$, (b) – $\overline{\sigma}_{yz}$.

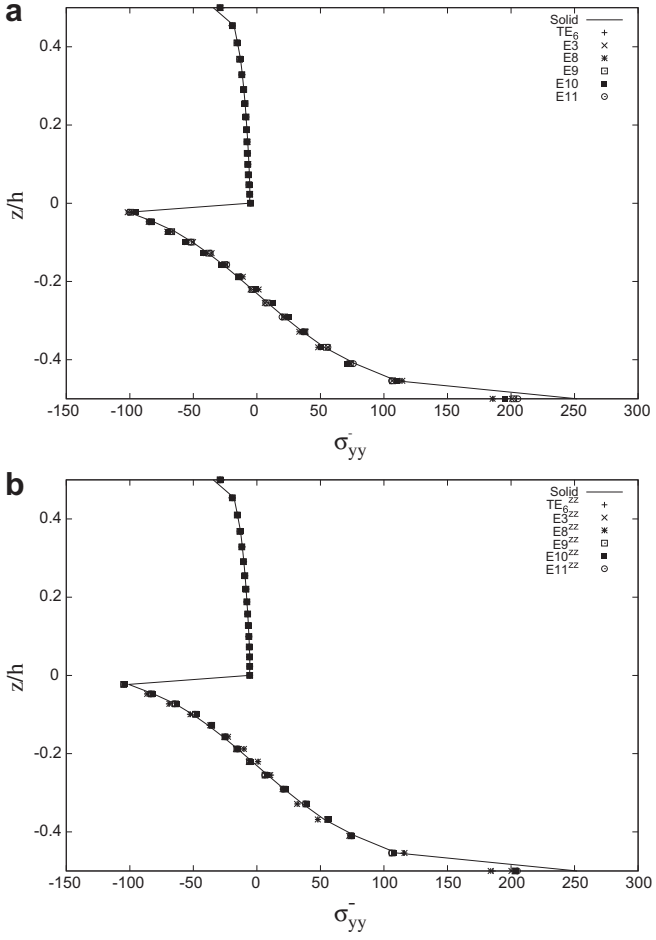

Fig. 8. Distribution of stresses $\overline{\sigma}_{yy}$ through-the-thickness of an anti-symmetric cantilever beam $(L/h = 4)$. (a) – $\overline{\sigma}_{yy}$, (b) – $\overline{\sigma}_{yy}$.

Pagano (1970) and Vidal and Polit (2011). Also in this case, it has to be noted that the results obtained with trigonometric and hyperbolic functions (see $E1$, $E3$, $E9$ and $E10$) are in strong agreement with the references. Furthermore comparing the results, the zig-zag function determines a large improvement of the solution both in terms of displacement and stresses.

The last tests involve two cantilever symmetric and antisymmetric laminated beams. The geometric characteristics are the same as the preceding case, but the Poisson ratios are assumed to be $\nu_{AT} = 0.1$ and $\nu_{TT} = 0.3$. These structures are subjected to a distributed load. The displacement of the tip, the stresses $\overline{\sigma}_{yy}$ and $\overline{\sigma}_{zz}$ are compared with those obtained by using the solid elements *HEX*20 of *MSC NASTRAN*© (Tables 10 and 11). First of all for both structures, it is interesting to note that the expansion $E8$, that employs the exponential functions, leads to results which are highly similar to the reference solution. With comparable number of degrees of freedom, the expansion $E1$ provides good results both in term of displacement and of longitudinal stress $\overline{\sigma}_{yy}$ whereas the stress $\overline{\sigma}_{zz}$ is not close enough to 1. Furthermore, in the last column of Table 10, the ratio between the CPU time related to the expansion and that one related to Euler-Bernoulli theory is shown. These values can give information about the real computational efforts that the refined theories require. Anyway, although the ratios can reach high values (200–300), with a common laptop, the computation time is around few tens of seconds. Again, the importance of the zig-zag function must be highlighted. In Figs. 5–10 the distributions through-the-thickness of the non-dimensional stresses

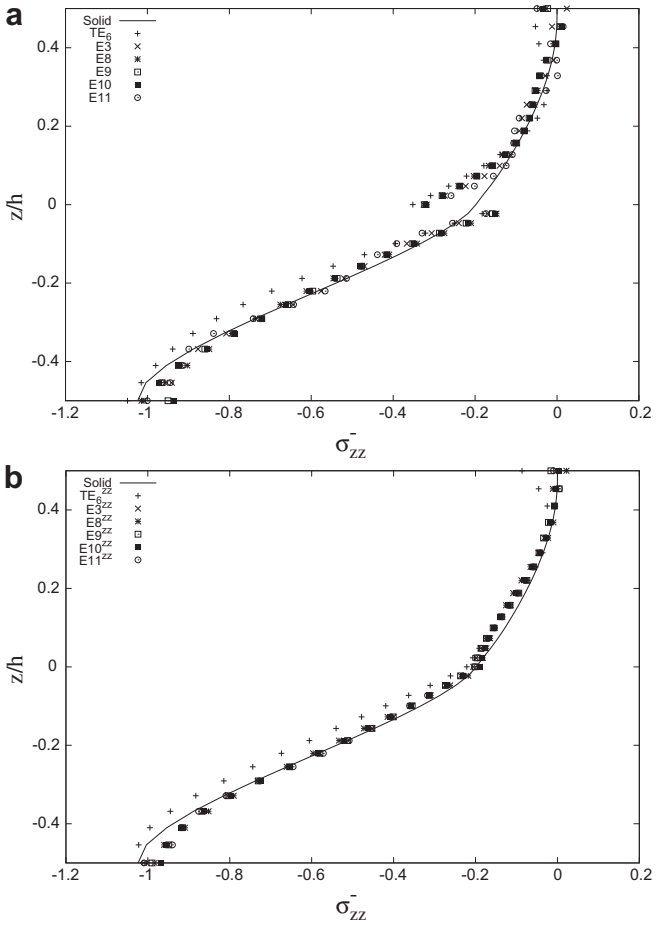

Fig. 9. Distribution of stresses $\overline{\sigma}_{zz}$ through-the-thickness of an anti-symmetric cantilever beam ($L/h = 4$). (a) $-\overline{\sigma}_{zz}$, (b) $-\overline{\sigma}_{zz}$.

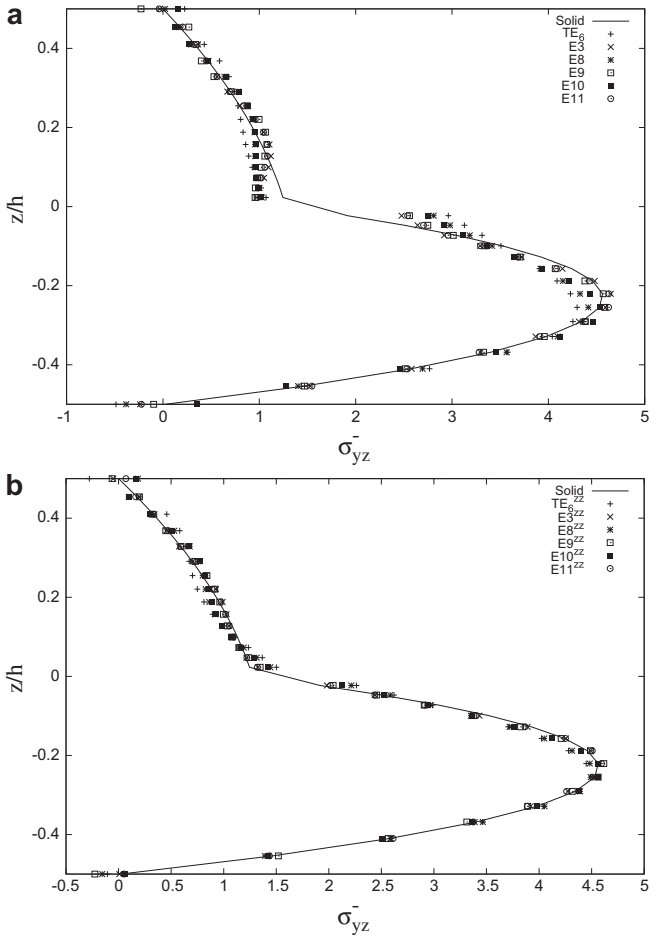

Fig. 10. Distribution of stresses $\overline{\sigma}_{yz}$ through-the-thickness of an anti-symmetric cantilever beam ($L/h = 4$). (a) $-\overline{\sigma}_{yz}$, (b) $-\overline{\sigma}_{yz}$.

($\overline{\sigma}_{yy}$, $\overline{\sigma}_{zz}$ and $\overline{\sigma}_{yz}$) are shown for several kinds of expansions. The figures labeled with (a) refer to the expansions without the zig-zag term whereas the other figures (b) show how the distributions are modified by the use of the aforementioned function. It is clear that the usage of the zig-zag function is more effective than increasing the orders used in the expansion of the variables. The possibility to combine a great number of functions by introducing the discontinuity of the first derivative of the displacements leads to quasi-3D solutions with low computational efforts.

5. Concluding remarks

In this work, the one-dimensional finite elements based on various displacement fields have been employed to perform static analyses of the laminated beams. The stacking sequences, the aspect-ratios and the boundary conditions have been considered as the problem parameters. The implementation of the finite elements have been carried out in accordance with Carrera's Unified Formulation. Several 1D models are able to obtain accurate solutions both in terms of displacement and stress distributions and, in the light of the results, the following final remarks can be made:

- For analyzing the composite beam, the use of refined 1D models is necessary in order to get acceptable results especially when thick structures are treated;
- The sinusoidal, hyperbolic and miscellaneous expansions are more effective than the other expressions for symmetric and

antisymmetric cross-ply beams for all load and boundary conditions;
- The exponential function becomes very important when the structure is cantilever;
- The zig-zag function substantially improves the solutions when symmetric and antisymmetric cross-ply beams are studied;
- The refined theories allow us to obtain quasi-3D solutions with a low number of DOFs.

Despite the difficulties to establish which functions are the best for the study of laminated beams, this paper demonstrates that the functions mentioned above are extremely effective. The results obtained indicate that these proposed higher-order theories are valuable for the investigation of the static behavior of composite beams and for this reason in future works, it will be very interesting to assess their capabilities by analyzing new static problems (for instance by considering different load conditions or laminated structures made up of layers with different Poisson's ratios) and the dynamic behavior of composites.

References

Ballhause, D., D'Ottavio, M., Kröplin, B., Carrera, E., 2004. A unified formulation to assess multilayered theories for piezoelectric plates. Computers and Structures 83, 1217–1235.

Bathe, K., 1996. Finite Element Procedure. Prentice Hall.

Carrera, E., 2002. Theories and finite elements for multilayered, anisotropic, composite plates and shells. Archives of Computational Methods in Engineering 9, 87–140.

Carrera, E., 2004. Assessment of theories for free vibration analysis of homogeneous and multilayered plates. Shock and Vibration 3–4, 261–270.

Carrera, E., 2003a. Historical review of zig–zag theories for multilayered plates and shells. Applied Mechanics Reviews 56, 287–309.

Carrera, E., 2003b. Theories and finite elements for multilayered plates and shells: a unified compact formulation with numerical assessment and benchmarking. Archives of Computational Methods in Engineering 10, 216–296.

Carrera, E., Giunta, G., 2010. Refined beam theories based on a unified formulation. International Journal of Applied Mechanics 2, 117–143.

Carrera, E., Petrolo, M., 2011. On the effectiveness of higher-order terms in refined beam theories. Journal of Applied Mechanics 78. http://dx.doi.org/10.1115/1.4002207.

Carrera, E., Boscolo, M., Robaldo, A., 2007. Hierarchic multilayered plate elements for coupled multifield problems of piezoelectric adaptive structures: formulation and numerical assessment. Archives of Computational Methods in Engineering 14, 383–430.

Carrera, E., Nali, P., Brischetto, S., 2008. Variational statements and computational models for multifield problems and multilayered structures. Mechanics of Advanced Materials and Structures 15, 182–198.

Carrera, E., Giunta, G., Nali, P., Petrolo, M., 2010. Refined beam elements with arbitrary cross-section geometries. Computers and Structures 88, 283–293. http://dx.doi.org/10.1016/j.compstruc.2009.11.002.

Carrera, E., Petrolo, M., Nali, P., 2011. Unified formulation applied to free vibrations finite element analysis of beams with arbitrary section. Shock and Vibration 18, 485–502. http://dx.doi.org/10.3233/SAV-2010-0528.

Carrera, E., Giunta, G., Petrolo, M., 2011. Beam Structures. Classical and Advanced Theories. Wiley.

Carrera, E., Filippi, M., Zappino, E. Numerical assessment of refined beam theories with various polynomial, trigonometric and exponential expansions over the cross-sections, submitted for publication.

Carrera, E., Petrolo, M., Zappino, E., 2012. Performance of CUF approach to analyze the structural behavior of slender bodies. Journal of Structural Engineering 138, 285–298.

Carrera, E., Petrolo, M., Wenzel, C., Giunta, G., Belouettar, S., Sept. 2009. Higher Order Beam Finite Elements With Only Displacement Degrees of Freedom, 1–11XIX Congresso AIMETA, Ancona (IT).

Carrera, E., Petrolo, M., Varello, A. Advanced beam formulations for free vibration analysis of conventional and joined wings, submitted for publication.

Carrera, E., Zappino, E., Filippi, M. Free vibration analysis of thin-walled cylinders reinforced with longitudinal and transversal stiffeners, in press.

Catapano, A., Giunta, G., Belouettar, S., Carrera, E., 2011. Static analysis of laminated beams via a unified formulation. Composite Structures 94, 75–83.

Davalos, J., Kim, Y., Barbero, E., 1994. Analysis of laminated beams with a layerwise constant shear theory. Composite Structures 28, 241–253.

Dufort, L., Drapier, S., Grdiac, M., 2011. Closed-form solution for the cross-section warping in short beams under three-point bending. Composite Structures 52, 233–246.

Euler, L., 1744. Theory of Elasticity. Bousquet, Lausanne and Geneva.

Giunta, G., Biscani, F., Belouettar, S., Ferreira, A., Carrera, E. Free vibration analysis of composite beams via refined theories, submitted for publication.

Giunta, G., Crisafulli, D., Belouettar, S., Carrera, E., 2011. Hierarchical theories for the free vibration analysis of functionally graded beams. Composite Structures 94, 68–74.

Grover, N., Maiti, D.K., Singh, B.N., 2013. A new inverse hyperbolic shear deformation theory for static and buckling analysis of laminated composite and sandwich plates. Composite Structures 95, 667–675.

Ibrahim, S., Carrera, E., Petrolo, M., Zappino, E., 2012. Buckling of composite thin walled beams by refined theory. Composite Structures 94, 563–570.

Jun, L., Hongxing, H., 2009. Dynamic stiffness analysis of laminated composite beams using trigonometric shear deformation theory. Composite Structures 89, 433–442.

Kapania, R.K., Raciti, S., 1989. Recent advanced in analysis of laminated beams and plates, part i: shear effects and buckling. AIAA Journal 27, 923–934.

Karama, M., Afaq, K., Mistou, S., 2003. Mechanical behaviour of laminated composite beam by the new multi-layered laminated composite structures model with transverse shear stress continuity. International Journal of Solids and Structures 40, 1525–1546.

Khdeir, A., 1996. Dynamic response of antisymmetric cross-ply laminated composite beams with arbitrary boundary conditions. International Journal of Engineering Science 34, 9–19.

Khdeir, A., Reddy, J., 1997a. Buckling of cross-ply laminate beams with arbitrary boundary conditions. Composite Structures 37, 1–3.

Khdeir, A., Reddy, J., 1997b. An exact solution for the bending of thin and thick cross-ply laminated beams. Composite Structures 37, 195–203.

Lekhniskii, S.G., 1968 (Translated from 2nd Russian). In: Tsai, S.W., Cheron, T. (Eds.), Anisotropic Plates. Gordon & Branch.

Mantari, J., Oktem, A., Soares, C.G., 2012. A new higher order shear deformation theory for sandwich and composite laminated plates. Composites: Part B 43, 1489–1499.

Matsunaga, H., 2002. Interlaminar stress analysis of laminated composite beams according to global higher-order deformation theories. Composite Structures 55, 105–114.

Murakami, H., 1986. Laminated composite theory with improved in-plane responses. Journal of Applied Mechanics 53, 661–666.

Novozhilov, V.V., 1961. Theory of Elasticity. Pergamon.

Onate, E.O., Eijo, A., Oller, S., 2012. Simple and accurate two-noded beam element for composite laminated beams using a refined zigzag theory. Computer Methods in Applied Mechanics and Engineering 213–216, 362–382.

Pagano, N., 1970. Exact solutions for rectangular bidirectional composites and sandwich plates. Journal of Composite Materials 4, 20–34.

Petrolo, M., Zappino, E., Carrera, E., 2012. Refined free vibration analysis of one-dimensional structures with compact and bridge-like cross-sections. Thin-Walled Structures 56, 49–61. http://dx.doi.org/10.1016/j.tws.2012.03.011.

Rao, M.K., Desai, Y., Chistnis, M., 2001. Free vibrations of laminated beams using mixed theory. Composite Structures 52, 149–160.

Reddy, J.N., 1984. A simple higher-order theory for laminated composites. Journal of Applied Mechanics 51, 745–752.

Reddy, J.N., 2004. Mechanics of Laminated Composite Plates and Shells. Theory and Analysis, second ed. CRC Press.

Shimpi, R.P., Ghugal, Y.M., 2001. A new layerwise trigonometric shear deformation theory for two-layered cross-ply beams. Composite Science and Technology 61, 1271–1283.

Shimpi, R.P., Ghugal, Y.M., 2002. A review of refined shear deformation theories of isotropic and anisotropic laminated plates. Journal of Reinforced Plastics and Composites 21, 775–813.

Surana, K., Nguyen, S., 1990. Two-dimensional curved beam element with higher-order hierarchical transverse approximation for laminated composites. Computers and Structures 36, 499–511.

Tahani, M., 2007. Analysis of laminated composite beams using layerwise displacement theories. Composite Structures 79, 535–547.

Tessler, A., Sciuva, M.D., Gherlone, M., 2009. A refined zigzag beam theory for composite and sandwich beams. Journal of Composite Materials 43, 1051–1081.

Timoshenko, S.P., 1921. On the correction for shear of the differential equation for transverse vibration of prismatic bars. Philosophical Magazine 41, 744–746.

Timoshenko, S.P., Goodier, J.N., 1970. Theory of Elasticity. McGraw-Hill.

Tsai, S.W., 1988. Composites Design, fourth ed. Think Composites, Dayton.

Vidal, P., Polit, O., 2008. A family of sinus finite elements for the analysis of rectangular laminated beams. Composite Structures 84, 56–72.

Vidal, P., Polit, O., 2009. Assessment of the refined sinus model for the non-linear analysis of composite beams. Composite Structures 87, 370–381.

Vidal, P., Polit, O., 2011. A sine finite element using a zig-zag function for the analysis of laminated composite beams. Composites: Part B 42, 1671–1682.

Vidal, P., Gallimard, L., Polit, O., 2012. Composite beam finite element based on the proper generalized decomposition. Computers and Structures 102–103, 76–86.

Vo, T.P., Thai, H.T., 2012. Static behavior of composite beams using various refined shear deformation theories. Composite Structures 94, 2513–2522.

Washizu, K., 1975. Variational Methods in Elasticity and Plasticity. Pergamon Press.

Xiaoshan Lin, Y.Z., 2011. A novel one-dimensional two-node shear-flexible layered composite beam element. Finite Elements in Analysis and Design 47, 676–682.